INTERNATIONAL SOCIETY FOR
SOIL MECHANICS AND
GEOTECHNICAL ENGINEERING

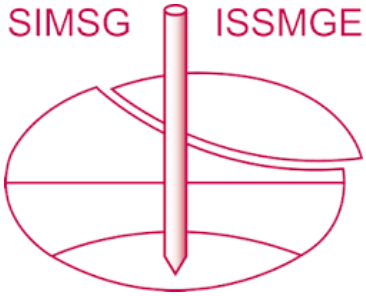

This paper was downloaded from the Online Library of the International Society for Soil Mechanics and Geotechnical Engineering (ISSMGE). The library is available here:

https://www.issmge.org/publications/online-library

This is an open-access database that archives thousands of papers published under the Auspices of the ISSMGE and maintained by the Innovation and Development Committee of ISSMGE.

Proceedings of the 16th International Conference on Soil Mechanics and Geotechnical Engineering
© 2005–2006 Millpress Science Publishers/IOS Press.
Published with Open Access under the Creative Commons BY-NC Licence by IOS Press.
doi:10.3233/978-1-61499-656-9-2391

Entrapment and dissolution behavior of DNAPL on subsurface contamination process

Le comportement de trappe et de dissolution de DNAPL sur le processus de contamination de couche superficielle

M. Kamon, T. Katsumi, T. Inui & K. Tsujimoto
Kyoto University, Japan
K. Endo
National Institute for Environmental Studies, Japan

ABSTRACT
The multiphase flow and contaminant transport analyses were conducted to examine the influence of the entrapment and dissolution behavior of DNAPL on the spatial distribution in the subsurface and its remedial efficiency by pump–and–treat method. Applicability of the full hysteresis model in DNAPL infiltration characteristics was verified by the result that dynamic DNAPL entrapment behavior (experimentally measured degree of DNAPL saturation) was properly quantified by the two phase flow numerical simulation. Also, analytical results on the DNAPL decontamination in the subsurface demonstrated that entrapment and rate-limited dissolution behavior of DNAPL are key factors of the remediation efficiency in the field.

RÉSUMÉ
Les études expérimentales et les analyses sur la multiphase écoulement et le transport de polluant à deux dimentions ont été faites pour examiner l'influence de comportement de la trappe et la dissolution de DNAPL a la distribution spatiale dans la couche superficielle et son efficacité remédiable par une méthode de pompe et traitement. Une application de modèle d'hystérésis complète aux caractéristiques d'infiltration de DNAPL a été vérifiée par un résultat tel que le comportement dynamique de trappe de DNAPL (degré de saturation de DNAPL mesuré expérimentalement) a été dien quantifié par une simulation numérique d'écoulement de deux phases. Aussi, les résultats analytiques sur la décontamination de DNAPL dans la couche superficielle ont démonstré que le comportement de la trappe et de la dissolution limitée à vitesse de DNAPL sont des facteurs importants d'efficacité remédiale dans les lieux.

1 INTRODUCTION

Volatile organic compounds (VOCs) such as trichloroethylene (TCE) or tetrachloroethylene (PCE) are known to exist in the contaminated subsurface as undiluted liquid called DNAPL (dense non-aqueous phase liquid) as well as vapor and solution. DNAPL could be retained in the pore space as a blob or a pool in the subsurface contamination process. DNAPL retained is generally referred to as residual DNAPL. Residual DNAPL becomes a persistent source of groundwater contamination due to its immobility and low solubility. Therefore, an evaluation of the mechanism for DNAPL migration is important in the site characterization from the aspects of DNAPL source volume and migration, as well as solute transport.

DNAPL retention characteristics in the saturated porous media are influenced by the physical properties of the porous media and the volume and pressure of released DNAPL. They could be described using a multiphase flow model, based on the relation among the capillary pressure head, which can be calculated by the difference between pore water and DNAPL pressures, and the degree of saturation (*S–p* relation). Hysteretic effects in the DNAPL infiltration lead to its retention in the porous media. Therefore, a consideration of the hysteresis in the *S–p* relation is essential for evaluating the DNAPL source migration. The rate-limited dissolution of DNAPL in the source zone to the water phase is another important factor, and may result in a persistent release of contaminants from DNAPL source. Theoretical estimations have been proposed to predict the dissolution mass transfer rate from the interfacial area of entrapped and continuous DNAPL and the system hydrodynamics. Also, laboratory-scale experiments have been conducted both in soil columns and larger scale systems, since the dissolution rate influences how long the release of DNAPL from its source/pool continues and the passive remedial action, such as pump-and-treat, should be kept effective.

In this paper, the entrapment behavior of DNPAL in the porous media was modeled using the numerical code which could account for the hysteretic effects in the *S–p* relation (Guarnaccia et al. 1998), and its reliability was verified by comparing to the profile of residual DNAPL obtained in the multiphase column tests under water-DNAPL two-phase system (Kamon et al. 2003). Furthermore, entrapment and dissolution behavior of DNAPL in the sandy medium containing the clay lens was analyzed to evaluate the spatial distribution in the subsurface and its remediation efficiency with the pump-and-treat method.

2 THEORY

2.1 *Hysteresis in the S–p relation*

Figure 1 shows the concept of the *S–p* relation under water-NAPL two-phase system, i.e. the relation among the degree of water saturation, S_W, and the capillary pressure head, h_{cNW} (= h_N – h_W) [L], where h_N [L] is the pore non-wetting phase pressure head and h_W [L] is the pore water pressure head. When the DNAPL infiltrates with a certain pressure in the water-saturated media (i.e. S_W = 1, h_{cNW} = 0), S_W and h_{cNW} shift along the PDC

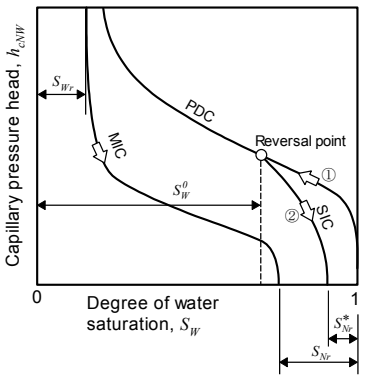

Figure 1. Concept of the full hysteresis in *S–p* relations.

(Primary Drainage Curve) to the reversal point, due to the infiltration pressure of DNAPL. When the DNAPL infiltration stops and the water starts to be supplied by the groundwater flow, S_W and h_{cNW} shift along the path, referred as to SIC (Scanning Imbibition Curve), from the reversal point. The endpoint of SIC, where h_{cNW} is equal to zero, does not coincide with the initial point (i.e. $S_W = 1$, $h_{cNW} = 0$) (Hilpert et al. 2001). S^*_{Nr} is generally defined as the effective residual DNAPL saturation, which is dependent on S^0_W, the water saturation at the reversal point (Land 1968). Numerical simulation in this study represents the entrapment of DNAPL in the water-DNAPL two-phase system by employing the hysteretic curve in the *S–p* relation and the parameter, S^*_{Nr}, shown in Fig. 1.

The *S–p* relation can be expressed by the following equation proposed by van Genuchten (1980).

$$h_{cNW} = \frac{1}{{}^x\alpha_{NW}}\left(S_e^{-1/m} - 1\right)^{1/n} \quad \text{where} \quad S_e = \frac{S_W - S_{Wr}}{1 - S_{Wr} - S^*_{Nr}} \tag{1}$$

where S_e is the effective saturation, S_{Wr} is the residual water saturation, ${}^x\alpha_{NW}$ [L^{-1}] ($x = d$; in the drainage process and $x = i$ in the imbibition process, generally ${}^i\alpha_{NW} = 2\,{}^d\alpha_{NW}$) and n [–] are the van Genuchten fitting parameters, and m is defined as $m = 1 - 1/n$. S^*_{Nr} can be expressed empirically as follows (Land 1968).

$$S^*_{Nr} = \frac{1 - S^0_W}{1 + R_N\,(1 - S^0_W)} \quad \text{where} \quad R_N = \frac{1}{S_{Nr}} - 1 \tag{2}$$

2.2 Dissolution of residual DNAPL

Dissolution behavior of residual DNAPL is affected by the flow velocity, the temperature, the DNAPL-water interfacial area, and so on. Laboratory experiments have been conducted to estimate the DNAPL-water mass transfer rate, as functions of DNAPL saturation, Reynolds Number, Schmidt number, molecular diffusion coefficient, and mean grain size of the concerned medium (e.g. Miller et al. 1990; Powers et al. 1994). To determine the DNAPL-water mass transfer rate, C^W_N [T^{-1}], this study employed the relationship expressed in Eq. (3), based on the laboratory experiments by Imhoff et al. (1992), designed to study dissolution kinetics of residual TCE in uniform sand.

$$C^W_N = \beta_1^{WN}\left(\varepsilon S_N\right)^{\beta_2}\left|v^W\right|^{\beta_3} \tag{3}$$

where β_1^{WN} is the rate coefficient for DNAPL-water mass transfer [T^{-1}], which is fit to available laboratory- or field-scale data, $\beta_2 \approx 0.5$ and $\beta_3 \approx 1.0$ are dimensionless fitting parameters, ε is the porosity of the porous medium, S_N is the DNAPL saturation, and v^W is the Darcy velocity vector of water [LT^{-1}].

3 ANALYSES ON THE MULTIPHASE COLUMN TEST

3.1 Modeling the DNAPL migration by the hysteretic S–p curve

To evaluate the hysteretic effects on the entrapment behavior of DNAPL, the one-dimensional infiltration of DNAPL in the saturated sandy medium was simulated, and the details were reported by Endo and Kamon (2003). In the simulation, numerical code developed by Guarnaccia et al. (1998) was employed under the boundary conditions in Fig. 2. Changes in DNAPL saturation with time at the middle of the column were calculated when the DNAPL or the water was induced from the top of column repeatedly every one hour. Table 1 shows the parameters used in the analyses. To model the entrapment of DNAPL, the hysteretic *S–p* curve, representing the hysteresis in both the drainage and the imbibition processes and the effective residual NAPL saturation, S^*_{Nr}, (Full Hysteresis Model, FHM) was employed. Also, Zero Hysteresis Model (ZHM), which considers no hysteresis in *S–p* curve, and Hysteresis Model (HM), which includes only the hysteresis between the drainage and the imbibition processes ($S^*_{Nr} = 0$), were employed to evaluate the hysteretic effects on the migration of DNAPL in the system.

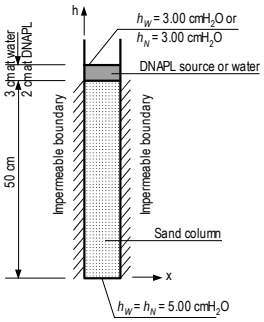

Figure 2. Boundary conditions for 1-D numerical analysis.

Table 1. Parameters used in the 1-D numerical analyses.

Parameter		Unit	Value
Intrinsic permeability	K	cm^2	1.0×10^{-7}
Porosity	n_s	–	0.40
Soil bulk density	ρ_d	g/cm^3	1.70
DNAPL Density	ρ_N	g/cm^3	1.50
Residual water saturation	S_{Wr}	–	0.15
Residual DNAPL saturation	S_{Nr}	–	0.30
VG: drainage α for air-water	${}^d\alpha_{NW}$	1/cm	0.020
VG: imbibition α for air-water	${}^i\alpha_{NW}$	1/cm	0.040
VG: parameter for soil	n	–	5.00

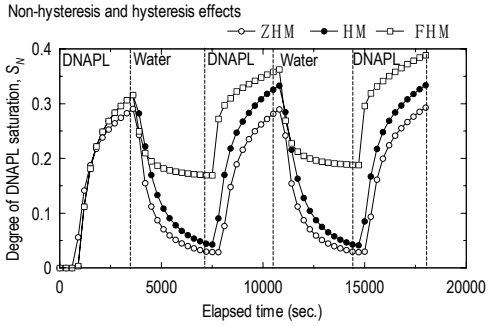

Figure 3. Hysteretic curve effects on DNAPL infiltration properties.

Figure 3 shows the profiles of DNAPL saturation with time, calculated with three different models (FHM, ZHM and HM). In the cases employing ZHM and HM, DNAPL saturation decreased to lower than 0.05 at the end of imbibition stage. In the case of FHM, entrapment of DNAPL was observed with its saturation of about 0.17 even at the end of the imbibition process. From these results, considering the effective residual DNAPL saturation in the hysteretic *S–p* curve has a significant effect on the entrapment volume of DNAPL.

3.2 Comparison with one-dimensional column experiments

To verify the reliability of the FHM as a method to simulate the entrapment of DNAPL in DNAPL-water two-phase system, the computational results on the DNAPL saturation were compared with the changes in DNAPL saturation measured using the multiphase column test (Kamon et al. 2003). Figure 4 shows the schematic diagram of the testing apparatus. Water-drainage and imbibition processes were alternately repeated (the steady-state flow was confirmed at the end of each process), and the changes in the degree of water saturation and the capillary pressure head were continuously measured. Three-electrode electrical probes were used to measure the degree of water saturation, and the hydrophilic and hydrophobic tensiometers were used to measure pore water and DNAPL pressure heads, respectively (Kamon et al. 2003). Hydrofluoroether (HFE-7100 produced by 3M^{TM}, DNAPL-water interfacial tension = 35.59 mN/m, relative density = 1.52, viscosity = 5.8×10^{-6} Pa·s) was used as the representative DNAPL. HFE has similar density and viscosity to TCE. Table 2 shows the parameters used in the analysis.

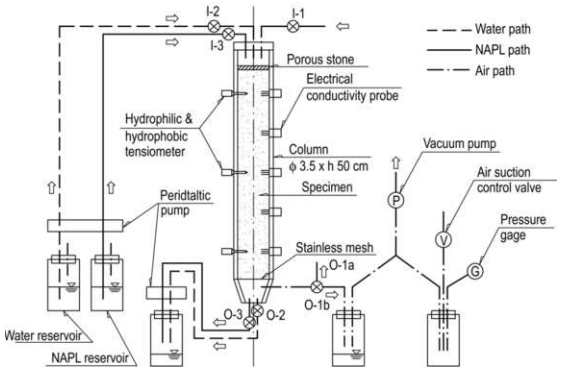

Figure 4. Apparatus for the multiphase column test (Kamon et al. 2003).

Table 2. Parameters used for simulating the multiphase column test.

Parameter		Unit	Value
Intrinsic permeability	K	cm^2	1.48×10^{-7}
Porosity	n_s	–	0.38
Soil bulk density	ρ_d	g/cm^3	1.63
DNAPL Density	ρ_N	g/cm^3	1.52
Residual water saturation	S_{Wr}	–	0.14*
Residual DNAPL saturation	S_{Nr}	–	0.49*
VG: drainage α for air-water	${}^d\alpha_{NW}$	1/cm	0.0212
VG: imbibition α for air-water	${}^i\alpha_{NW}$	1/cm	0.0424
VG: parameter for soil	n	–	6.57*

* Values experimentally determined based on Kamon et al. (2003)

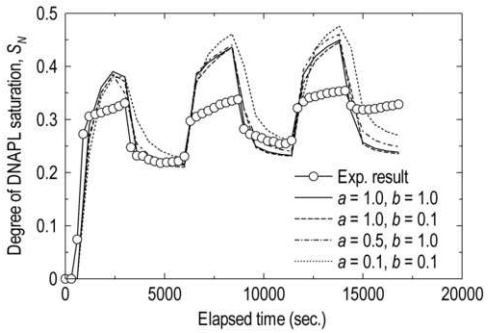

Figure 5. Experimental vs. analytical results on DNAPL saturation.

Figure 5 shows both experimental and simulated results on the changes in DNAPL saturation, S_N, with time under the repeated water-drainage and imbibition processes, with the suction of 1.94 kPa supplied at the bottom of the column. The blending parameters of a and b shown in the caption are related to the entrapment rate of DNAPL in the porous media (Guarnaccia et al. 1998). Analytical results using FHM could simulate the entrapment behavior of HFE in the water-imbibition process accurately, although it overestimated the increasing of S_N in the water-drainage process. Combined with the results on Fig. 3, it can be concluded that the FHM can simulate the entrapment behavior of DNAPL in the saturated porous media rather than other models (ZHM and HM).

4 ANALYSES ON THE TCE DISTRIBUTION IN THE SUBSURFACE AND ITS REMEDIATION

To evaluate the effects of the entrapment and dissolution behavior of DNAPL on the distribution in the subsurface and its recovery efficiency with the pump-and-treat method, numerical analyses were performed using the finite difference code by Guarnaccia et al. (1998). In these analyses, the FHM and the dissolution of DNAPL based on Eq. (3) were considered to simulate both the TCE infiltration/entrapment and the advective-dispersive transport of dissolved TCE in the aquifer. Figure 6 shows the cross section for numerical analyses (40 m width × 20 m depth) and boundary conditions. Fully saturated sandy medium containing a clay lens (10 m width × 2 m thickness) was considered as the analytical domain. The bottom boundary was composed with the clay layer. Table 3 shows the parameters used in numerical analyses, related to the physical properties of sand and clay layers, and the characteristics of TCE infiltration and dispersive transport. Lateral groundwater flow with the hydraulic gradient of 0.01 was supplied by fixing 40 cm H_2O pressure head at the left-hand side boundary for the water phase. It was assumed that TCE was spilled into the sandy medium with the rate of 0.1 cm^2/s for 72 hours at the spillage point shown in Fig. 6. Spatial distribution of TCE was simulated i) in 40 years without any remediation after the spillage stopped and ii) in 38 years with the pump-and-treat followed by the DNAPL migration in 2 years after the spillage stopped (totally 40 years). In the pump-and-treat process, it was assumed that TCE was recovered from different recovery wells (Well-1 and -2; 10 m and 15 m away horizontally from the spillage point, respectively) with different pumping rates of 6.0 and 3.0 cm^2/s. Main emphasis was placed upon the recovery efficiency of the residual and dissolved TCE in the aquifer.

The analytical results at (a) 2 years after the spillage and (b) 10 years after the pump-and-treat with the rate of 6.0 cm^2/s started are shown in Fig. 7 with respect to the degree of TCE saturation. Figure 7 (a) indicates that TCE was infiltrated downward from the spillage point, reached the top surface of clay lens, and migrated laterally along the top surface of clay lens. Only little portion of TCE infiltrate into the clay lens due to its entry pressure. The maximum degree of TCE saturation above the clay lens was approximately 0.10. Along with the infiltration path, entrapment of TCE was observed. Figure 7 (b) indicates that the total volume of residual TCE was significantly reduced by the pumping for 10 years, although TCE was retained in the domain where the high degree of TCE saturation was observed initially (see Fig. 7 (a)). Residual TCE also ex-

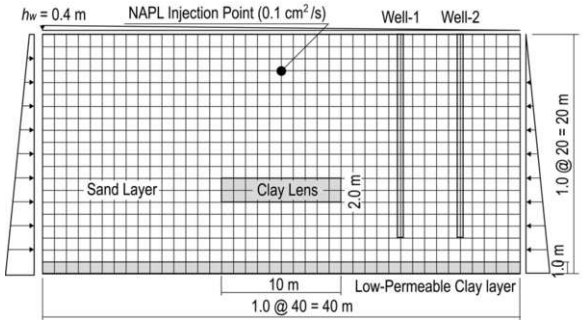

Figure 6. Cross section for 2-D numerical analysis.

Table 3. Parameters used in the 2-D numerical analyses.

Parameters for soil		Unit	Value	
			Sand	Clay
Intrinsic permeability	K	cm^2	2.0×10^{-7}	1.8×10^{-9}
Porosity	n_s	–	0.40	0.40
Soil bulk density	ρ_d	g/cm^3	1.70	1.50
Residual water saturation	S_{Wr}	–	0.15	0.20
Residual TCE saturation	S_{Nr}	–	0.35	0.30
VG: drainage α for air-water	${}^d\alpha_{NW}$	1/cm	0.026	0.009
VG: imbibition α for air-water	${}^i\alpha_{NW}$	1/cm	0.052	0.017
VG: parameter for soil	n	–	5.6	3.2
Parameters for TCE		Unit	Value	
Density	ρ	g/cm^3	1.456	
Viscosity	μ	Pa·s	0.0056	
Surface tension	σ_{NA}	mN/m	29.3	
Interfacial tension	σ_{NW}	mN/m	34.5	
Solubility limit	ρ_{Wmax}	mg/m^3	1.00	
Dissolution rate coefficient	β_1^W	1/s	1.75×10^{-3}*	
Longitudinal dispersion length	α_L	cm	10.0	
Transverse dispersion length	α_T	cm	1.0	
Diffusion coefficient in water	D^{WN}	cm^2/s	1.00×10^{-5}	

* by Schaerlaekens et al. (2000)

isted at the sides of the clay lens where the flow velocity was relatively low. These observations support that the heterogeneity in the porous media significantly influences the spatial distribution of TCE in both infiltration and recovery processes.

The analytical result at 10 years after the pump-and-treat with the rate of 6.0 cm^2/s started at Well-1 is shown in Fig. 8 with the respect to the concentration of TCE in aqueous phase. In the domain around the well, where the flow velocity was relatively high with the pumping effect, higher TCE concentrations were observed. The higher flow velocity leads to the higher dissolution rate of TCE in accordance with Eq. (3), and promotes the recovery of TCE by pumping close to the TCE source. Figure 9 (a) shows the profile of the total volume of residual TCE with time during the pump-and-treat, compared with the one without any remediation. In the case of the pumping with the rate of 6.0 cm^2/s at Well-1, volume of residual TCE was linearly reduced till 20 years after, however, the efficiency of TCE recovery was very low after that and a low level of residual TCE existed persistently. Computational results revealed that most of residual TCE after 20 years existed around and inside the clay lens where the flow velocity was relatively low, since the residual TCE is difficult to be replaced with the water phase and subjected to the lower dissolution rate. From these observations, the heterogeneity leads to the persistent groundwater contamination even when its recovery is continuously conducted near the DNAPL source. In the cases of the pumping with the lower rate (3.0 cm^2/s) or at the well further from the source (Well-2), the recovery efficiency is drastically lowered. Figure 9 (b) shows the changes in TCE concentrations in the pumped water with time, during the pump-and-treat at Well-1 with different rates. TCE concentrations are consistent with the recovery efficiency, which is regarded as the gradient of total volume reduction of residual TCE shown in Fig. 9 (a). Particularly, TCE concentrations in the case of lower pumping rate (3.0 cm^2/s) are almost constant even 40 years after, which implies that the pump-and-treat should be adopted persistently when the pumping rate is limited.

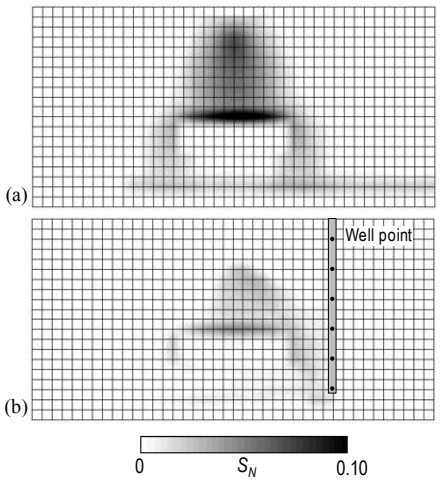

Figure 7. Computational results on the degree of TCE saturation: (a) 2 years after the spillage and (b) 10 years after the pump-and-treat started.

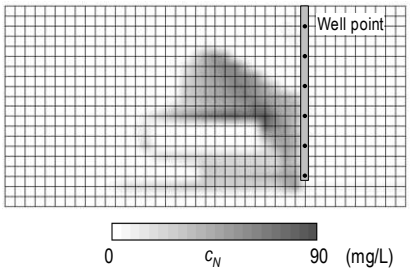

Figure 8. Computational results on dissolved TCE concentrations: 10 years after the pump-and-treat started.

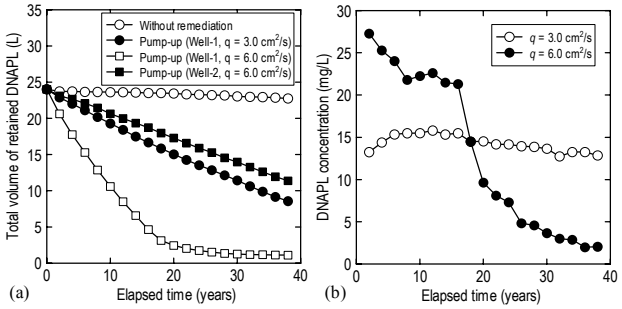

Figure 9. Profiles of (a) residual TCE volume and (b) TCE concentration in pumped water with time.

5 CONCLUSIONS

In this paper, the reliability of employing the hysteretic *S–p* curve, including the hysteresis in both the water-drainage and imbibition processes and the effective residual DNAPL saturation (Full Hysteresis Model), as a method for evaluating the entrapment behavior of DNAPL in the subsurface was verified by comparing the degree of DNAPL saturation measured in the multiphase column infiltration test. FHM was able to evaluate successfully the entrapment of DNAPL in the water-imbibition process. To evaluate the effects of the entrapment and dissolution behavior of DNAPL on the spatial distribution in the subsurface and its recovery efficiency with the pump-and-treat method, numerical analyses were performed for two-dimensional heterogeneous porous medium. Numerical analyses simulated the effects of the heterogeneity on the persistency of the groundwater contamination and its recovery due to the residual DNAPL. From these observations, the volume of the residual DNAPL and its dissolution rate are key factors in the site characterization on the groundwater contamination by DNAPL, and their evaluation is essential in designing the remediation.

REFERENCES

Endo, K. and Kamon, M (2003): Hysteretic curve effects for residual DNAPL, *Proceedings of the 38th Japan National Conference on Geotechnical Engineering*, 2377-2378 (in Japanese).

Guarnaccia, J. et al. (1998): *NAPL: Simulator Documentation*, EPA/600/R-97/102, U.S.EPA.

Hilpert, M. et al. (2001): Investigation of the residual-funicular nonwetting-phase-saturation relation, *Advances in Water Resource*, 24, 157-177.

Imhoff, P.T. et al. (1992): An Experimental Study of the Dissolution of Trichloroethylene in Saturated Porous Media, *Princeton University Water Resources Program Report*, WR-92-1.

Kamon, M. et al. (2003): Measuring the *k–S–p* relations on DNAPLs migration, *Engineering Geology*, 70, 351-362.

Land, C.S. (1968): Calculation of imbibition relative permeability for two- and three-phase flow from rock properties, *Trans. Am. Inst. Min. Metall. Pet. Eng.*, 243, 149-156.

Miller, C.T. et al. (1990): Dissolution of trapped nonaqueous phase liquids: mass transfer characteristics, *Water Resources Research*, 26, 2783-2796.

Powers, S.E. et al. (1994): An experiment investigation of nonaqueous phase liquid dissolution in saturated subsurface systems: transient mass transfer rates, *Water Resources Research*, 30, 321-332.

Schaerlaekens, J. et al. (2000): Surfactant enhanced solubilization of residual trichloroethene: An experimental and numerical analysis, *Journal of Contaminant Hydrology*, 46, 1-16.

van Genuchten, M.Th. (1980): A closed-form equation for predicting the hydraulic conductivity of unsaturated soils, *Soil Science Society of America Journal*, 44, 892-898.